Enzyme Kinetics

Deutsche Ausgabe: DOI: 10.1002/ange.201511985
Internationale Ausgabe: DOI: 10.1002/anie.201511985

Commercial Herbicides Can Trigger the Oxidative Inactivation of Acetohydroxyacid Synthase

Thierry Lonhienne, Amanda Nouwens, Craig M. Williams, James A. Fraser, Yu-Ting Lee, Nicholas P. West, and Luke W. Guddat**

Abstract: *Acetohydroxyacid synthase (AHAS) inhibitors are highly successful commercial herbicides. New kinetic data show that the binding of these compounds leads to reversible accumulative inhibition of AHAS. Crystallographic data (to a resolution of 2.17 Å) for an AHAS–herbicide complex shows that closure of the active site occurs when the herbicidal inhibitor binds, thus preventing exchange with solvent. This feature combined with new kinetic data shows that molecular oxygen promotes an accumulative inhibition leading to the conclusion that the exceptional potency of these herbicides is augmented by subversion of an inherent oxygenase side reaction. The reactive oxygen species produced by this reaction are trapped in the active site, triggering oxidation reactions that ultimately lead to the alteration of the redox state of the cofactor flavin adenine dinucleotide (FAD), a feature that accounts for the observed reversible accumulative inhibition.*

Acetohydroxyacid synthase (AHAS; EC 2.2.1.6), the first enzyme in the branched chain amino acid biosynthesis pathway, catalyzes either the conversion of two molecules of pyruvate into 2-acetolactate, or one molecule of pyruvate and one molecule of 2-ketobutyrate to 2-aceto-2-hydroxybutyrate (Figure 1). This enzyme is found in plants, bacteria, and fungi but not in animals, making it an attractive target for biocide discovery. Indeed, inhibitors of AHAS have been highly successful commercial herbicides for more than thirty years.[1] However, a lack of clarity surrounds the mechanism of inhibition of AHAS by these herbicides. The reaction has been reported to be time-dependent and biphasic,[2] corresponding to slow-binding inhibition. However, in AHAS, this process has only been observed under turnover conditions,[3] suggesting that there may be an alternative explanation for the observed time-dependent and biphasic inhibition profiles. Adding to the conjecture, the inhibition of AHAS by herbicides has, in some cases, been reported to be irreversible,[2a,4] which is inconsistent with a mechanism of slow-binding inhibition. In addition, it is also feasible that thiamin diphosphate (ThDP; a Breslow intermediate), a cofactor in the active site, can participate in alternative reactions with the herbicide (for example by protonation of the enamine or by formation of the keto form through tautomerization),[5] thereby influencing inhibition.

Herein, we report our investigations into the process of AHAS inhibition at suboptimal concentrations using penoxsulam (PS; Figure 1B), as a lead example of the triazolopyrimidine sulfonamide family of herbicides. The kinetic curves (Figure 2A) resemble those reported previously for inhibitors of AHAS where the time dependence of the inhibition was accredited to reversible slow-binding inhibition.[2c,6] However, in this case, slow-binding inhibition is not involved because the amount of inhibition of AHAS at low concentrations of inhibitor exceeds stoichiometric equivalence. For example, at a concentration of 25 nM, PS inactivated approximately 1 μM of *Saccharomyces cerevisiae* AHAS (*Sc*AHAS) within 50 min (Figure 2A, curve e). Thus, the time dependence of the inhibition can only be attributed to accumulative inactivation of *Sc*AHAS. The activity did not decrease to zero, but reached a steady state that was inversely proportional to the concentration of the inhibitor (Figure 2A, curves b–f), suggesting that inactivated *Sc*AHAS was able to recover activity. An enzyme-inhibitor dilution experiment confirmed this aspect of the inhibition by showing that within 80 min, about 65% of inactivated *Sc*AHAS recovers activity (Figure 2B), suggesting that the time-dependent inhibition detected is fully reversible, if given enough time.

To adequately fit the data, a model representing the mechanism of inhibition was established (Figure 2C) and the following equation was derived (see the Supporting Information for equation derivation):

$$[\mathrm{P}] = V_{\max}\left(\mathrm{F}\left(\frac{k_3}{k_{\mathrm{iapp}} + \mathrm{F}k_3}\right)t + \left(\frac{k_{\mathrm{iapp}}}{k_{\mathrm{iapp}} + \mathrm{F}k_3}\right)\frac{1}{(k_{\mathrm{iapp}}/\mathrm{F} + k_3)}\left(1 - \exp\left[-\left(\frac{k_{\mathrm{iapp}}}{\mathrm{F}} + k_3\right)t\right]\right)\right) \quad (1)$$

The equation includes two variable parameters: k_{iapp} representing an apparent first-order rate of inhibition, and k_3 representing a first-order rate of recovery of the native enzyme (reversal rate). The parameter F is the fraction of total enzyme concentration versus the total concentration of inhibitor, $V_{\max}$ is the maximum velocity rate of substrate disappearance measured in the absence of inhibitor, and P is the reaction product. The equation was used to fit the experimental curves (see the Supporting Information), giving an average k_{iapp} value of $2.7 \pm 0.3\ \mathrm{min}^{-1}$ (SEM, standard error of the mean) and a k_3 value estimated at $0.01\ \mathrm{min}^{-1}$.

[*] Dr. T. Lonhienne, Dr. A. Nouwens, Prof. C. M. Williams, Prof. J. A. Fraser, Y. Lee, Dr. N. P. West, Prof. L. W. Guddat
School of Chemistry and Molecular Biosciences
The University of Queensland
Brisbane, 4072 QLD (Australia)
E-mail: t.lonhienne@uq.edu.au
luke.guddat@uq.edu.au

Supporting information and the ORCID identification number(s) for the author(s) of this article can be found under http://dx.doi.org/10.1002/anie.201511985.

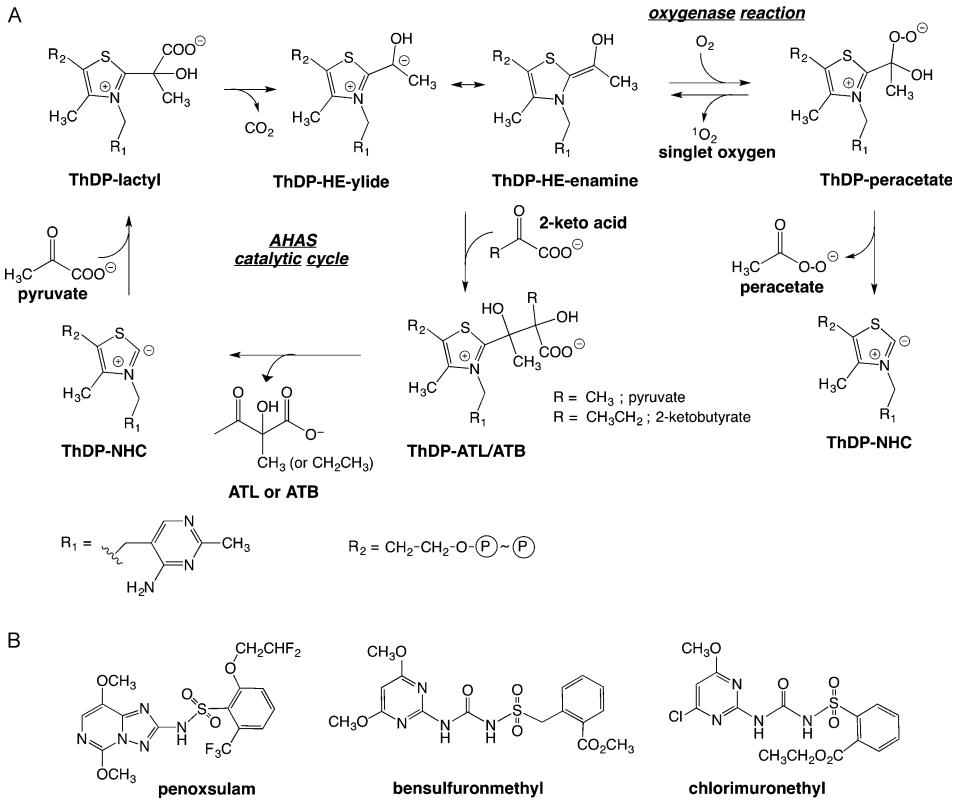

Figure 1. Reactions and inhibitors of AHAS. A) Reactions catalyzed by AHAS including the catalytic cycle and the oxygenase side reaction. B) Structures of three AHAS inhibitors. ThDP = thiamin diphosphate; HE = hydroxyethyl; ATL = acetolactate; ATB = acetohydroxybutyrate; NHC = N-heterocyclic carbene.

To assess the generality of the mechanism of inhibition observed with PS, bensulfuron methyl (BSM; Figure 1 B), a sulfonylurea inhibitor having a high affinity for *Sc*AHAS,[7] was also assayed. BSM has a similar rate of inhibition compared to PS with a k_{iapp} value of $1.9 \pm 0.4\ min^{-1}$. However, the k_3 value is lower, estimated to be $0.004\ min^{-1}$ (see Figure S1 A in the Supporting Information). Given the chemical structures of PS and BSM are markedly different, these results suggest that accumulative inhibition of AHAS by commercial herbicides from these families is a common phenomenon. Inhibition assays of *Mycobacterium tuberculosis* AHAS (*Mt*AHAS) with PS also showed accumulative inhibition, although to a lesser extent, with a k_{iapp} value of $1 \pm 0.2\ min^{-1}$ and a k_3 value of $0.03\ min^{-1}$ (Figure S1 B). These results show that the parameters that define accumulative inhibition are variable, reflecting differences in specific structural features of the individual inhibitors and enzymes.

To determine whether turnover is a prerequisite for accumulative inhibition to occur, *Sc*AHAS (13 μM) was incubated for 160 min with PS (0.2 μM), with or without the addition of pyruvate. The incubation was carried out on ice in order to significantly reduce turnover and to ensure that pyruvate remained present throughout the experiment. Measurement of enzyme activity over time (see the Supporting Information) showed that pyruvate is required for time-dependent inhibition to occur (Figure 2 D). Noticeably, in the absence of pyruvate, there is an initial inhibition present that persists affecting about 25% of the enzyme. An explanation for this result is that a portion of the enzyme preparation contains a form highly prone to accumulative inhibition, potentially when ThDP-HE (Figure 1) is bound. The requirement of turnover conditions suggests that binding to a specific catalytic intermediate is required for the herbicide to be able to trigger this mode of inhibition. This is in agreement with the theory of Schloss[8] in which the stabilization of the ThDP-HE intermediate is the factor that triggers irreversible inhibition. Schloss proposed the following mechanism: the binding of the inhibitor to the ThDP-HE intermediate (Figure 1) holds the enzyme in an oxygen-sensitive state that is prone to reaction with molecular oxygen (O_2), forming a peracetate adduct. The reactive oxygen species (ROS) produced by decomposition of the peracetate adduct[9] (that is, peracetate or singlet oxygen; see Figure 1 A) are then trapped on the enzyme by the herbicide, increasing the likelihood of oxidative inactivation of the enzyme.

Features that correspond to this mechanism are detected in the crystal structure of *Sc*AHAS in complex with BSM (2.17 Å resolution; Table S1). The structure shows that conformational changes occur upon binding of BSM to *Sc*AHAS that no longer allow pyruvate access to ThDP-HE (Figure 3). As a result, electrophilic attack by O_2 can then occur without competition by pyruvate. Under such conditions our hypothesis is that the concentration of dissolved O_2, acting as a substrate for the oxygenase reaction, should affect the rate of accumulative inhibition. We have confirmed this by purging the mixture with argon prior to assaying. This pretreatment results in an overall decrease in the steady state of inhibition (Figure S2) and supports a mechanism in which the production of ROS by the oxygenase side reaction is at the core of the accumulative inhibition. As the conformation taken by AHAS in complex with the inhibitor occludes the active site from solvent (Figure 3), the ROS are trapped and are therefore unable to react with pyruvate as occurs under normal conditions of catalysis,[2b] reacting instead with components of the enzyme (for example FAD). Based on these results, we next set out to investigate how this oxidation could be responsible for the reversible accumulative inhibition detected in our system.

Tittmann et al.[10] demonstrated that enzyme-bound FAD in AHAS is reduced during catalysis in a side reaction that oxidizes pyruvate into acetate and carbon dioxide. Therefore,

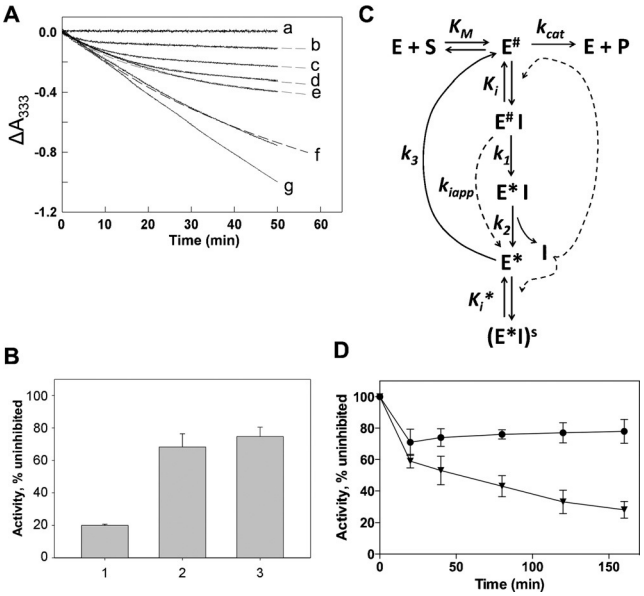

Figure 2. Time-dependent inhibition of *Sc*AHAS by penoxsulam (PS). A) Progress curves for inhibition. 1.2 μM *Sc*AHAS was assayed at 20 °C in 200 mM potassium phosphate (pH 7.2) containing 10 mM $MgCl_2$, 1 mM ThDP, 10 μM FAD, and 100 mM pyruvate and varying concentrations of PS (curves a–g correspond to assays containing 1.2, 0.1, 0.05, 0.036, 0.025, 0.01, and 0 μM of PS, respectively). Specific activities of the enzyme after 50 min of incubation were 0 (curve a), 0.25 (b), 0.5 (c), 0.75 (d), 1 (e), 3.7 (f), and 6.3 U mg^{-1} (g), respectively. The experimental data (curves b–f) were fitted using Equation (1), giving inhibition rates (k_{iapp}) of 3.06, 2.75, 2.38, 2.9, and 2.47 min^{-1}, respectively. B) Recovery of *Sc*AHAS activity by a dilution experiment. 2.1 μM *Sc*AHAS in solution in standard buffer was incubated on ice for 3 h, with (experimental sample) or without (control sample) addition of 0.04 μM PS in standard buffer, leading to an 80% loss of enzyme activity in the experimental sample (column 1). Aliquots of both treatments were then diluted 500-fold in buffer, with or without the addition of 100 mM pyruvate, and incubated at 20 °C for 80 min. Under these conditions, the final concentration of inhibitor was 0.08 nM, a value well below the K_i value. In the diluted control samples, 0.08 nM PS was added to take into account the residual presence of PS in the diluted experimental samples. The measurement of the residual activity showed that *Sc*AHAS had recovered around 65% of its activity during the dilution treatment (60% recovered in the absence of pyruvate (column 2), 68% in the presence of pyruvate (column 3)). C) Model for time-dependent accumulative inhibition. E = free enzyme, K_M = Michaelis constant for the substrate (S), $E^{\#}$ = enzyme in reaction with S, I = inhibitor, E* = inactivated enzyme, K_i = dissociation constant between I and $E^{\#}$, K_i* = dissociation constant between I and E*, k_1 = intrinsic first-order rate constant of enzyme inactivation, k_2 = first-order rate constant for the dissociation of the complex E*I, k_{iapp} = apparent rate of inactivation, k_3 = reversal first-order rate constant, and k_{cat} = catalytic rate constant. D) Effect of pyruvate on the kinetics of inhibition of *Sc*AHAS by PS. 13 μM of *Sc*AHAS was incubated at 0 °C with all cofactors and 0.2 μM PS in the absence (▼) or presence (●) of pyruvate. Aliquots were taken over time, and diluted 1000-fold in standard buffer. Initial velocities were monitored using the discontinuous method (see the Supporting Information).

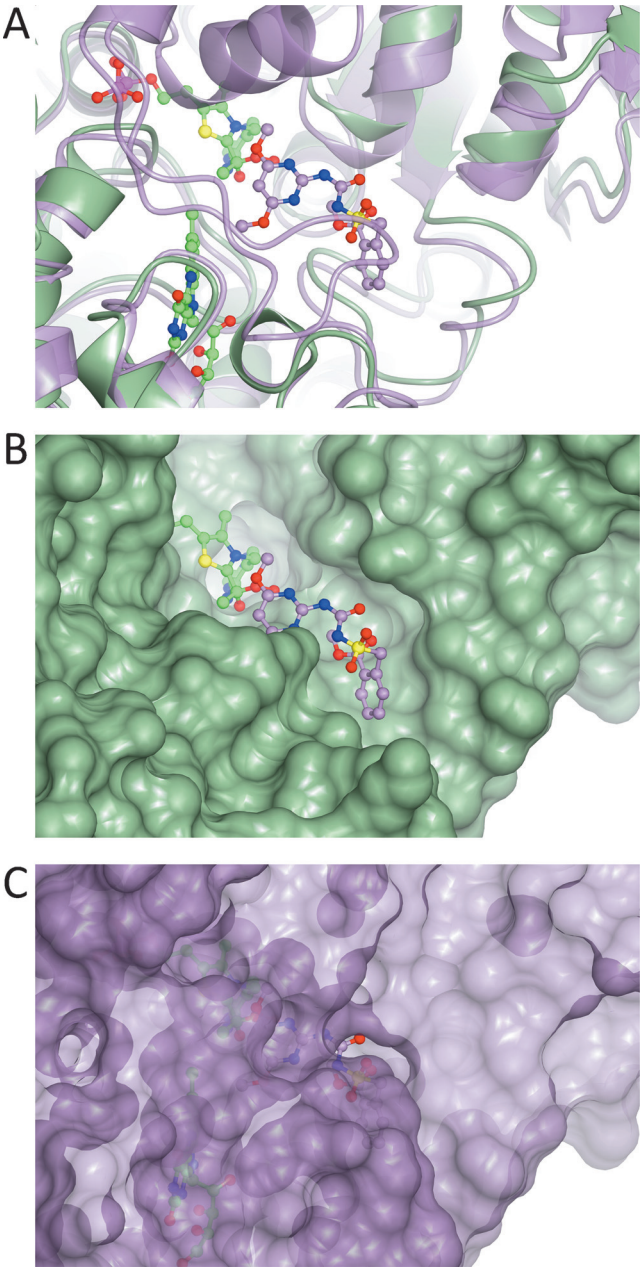

Figure 3. Comparison of the crystal structure of the *Sc*AHAS–BSM complex with the free enzyme. A) Superimposition of the free enzyme (PDB code 1JSC; green) with the *Sc*AHAS–PS complex (lilac). B) BSM artificially superimposed onto the surface of the free enzyme. C) The surface (partially transparent) of the *Sc*AHAS–BSM complex with BSM partially visible. Upon formation of the complex, there is movement of the α-domain toward the γ-domain of the opposing subunit (top-right in (A)), ordering of two regions of the polypeptide (E579–Y595 and K648–H687, dark purple; bottom-left in (C)), and formation of two α-helices (Q580–Y591 and P669–T683; top-left in (A)).

the redox status of enzyme-bound FAD was monitored during accumulative inhibition. At 15 °C, after a lag-phase period of 25 min, both the catalytic activity and the FAD absorbance reached a steady state that lasted for an additional 25 min (Figure 4 A,B, curve a).

The UV/Vis absorbance spectra of *Sc*AHAS prior to substrate turnover revealed a typical absorbance profile for oxidized FAD, with two bands at $\lambda \approx 378$ and 450 nm (Figure 4 C). The 450 nm band was not present when the enzyme was under turnover conditions in the steady state, implying that FAD had been fully reduced during the lag phase

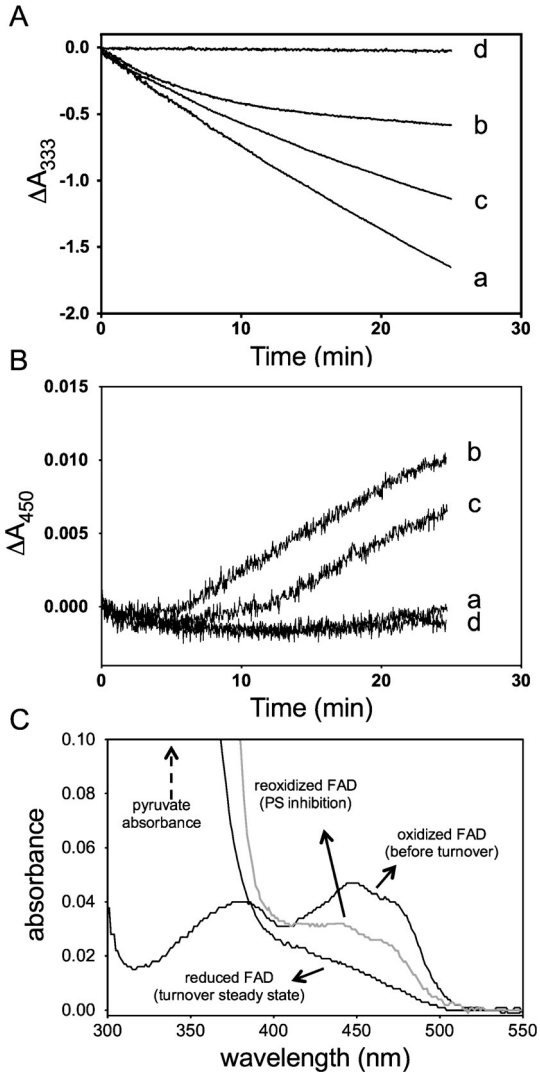

Figure 4. Accumulative inhibition of *Sc*AHAS is accompanied by oxidation of enzyme-bound FAD. A, B) Progress curves of *Sc*AHAS activity in the presence of pyruvate and monitored at A) $\lambda = 333$ nm and B) 450 nm (intrinsic absorbance of FAD). 5.5 μM *Sc*AHAS–FAD was incubated at 15 °C in buffer containing 200 mM potassium phosphate buffer (pH 7.2), 160 mM pyruvate, 1 mM ThDP, and 10 mM Mg^{2+}, without inhibitor (curve a), with 0.5 (curve b) or 0.25 μM PS (curve c), or with 10 μM chlorimuron ethyl (CE; curve d). Monitoring of the progress curves started after 25 min of reaction corresponding to the time necessary to reach the turnover steady state. Inhibitors were added at the start of the monitoring. C) UV/Vis absorbance spectra of *Sc*AHAS before turnover, during the turnover steady state, and after 25 min of inhibition with 0.5 μM PS.

(Figure 4C). However, PS added to the assay mixture at the start of the steady state triggered a gradual re-oxidation of FAD, in proportion with the concentration of the inhibitor (Figure 4A, B). CE, a sulfonylurea inhibitor of *Sc*AHAS,[11] did not show accumulative inhibition in our assays and did not alter the redox status of FAD, implying that re-oxidation of FAD is specifically linked to accumulative inhibition.

This result agrees with studies in our laboratory showing that *Sc*AHAS activity is closely linked to the redox status of enzyme-bound FAD in that, in order to be active, the enzyme strictly requires FAD to be reduced. Therefore, it suggests that the process of oxidation of FAD by ROS relates to the rate of accumulative inhibition, whereas the re-reduction of FAD through pyruvate oxidase (POX) activity[10] relates to the rate of recovery of activity, accounting for the reversibility of accumulative inhibition. Importantly, the rate constant of the POX side reaction in *Ec*AHAS II is lower than the rate constant of the AHAS reaction by two orders of magnitude.[10] This explains how the process of oxidation of FAD is at least partially involved in the process of accumulative inhibition. However, it cannot be excluded that indirect oxidation of $FADH_2$ by ROS is involved in the mechanism of reversible accumulative inhibition.

The data presented herein brings new insights into the mode of action of herbicidal inhibitors of AHAS. We propose that the slow-binding inhibition reported previously corresponds to the accumulative inhibition demonstrated herein. Furthermore, accumulative inhibition offers a comprehensive explanation of all of the available experimental data. First, the requirement for turnover conditions in accumulative inhibition is logically explained by the fact that the binding of the inhibitor to the AHAS ThDP–HE catalytic intermediate is the critical event leading to oxidative inactivation of the enzyme. There is no equivalent logical explanation for slow-binding inhibition. Second, although slow-binding inhibition is in theory a reversible process,[2c] in some cases, it has been reported to be accompanied by partial or complete irreversible inactivation of AHAS.[12] Accumulative inhibition rationalizes the inconsistencies in previously reported analyses of the data. The variability of the rate of recovery of native enzyme (k_3) values obtained with the accumulative inhibition model (this study, 0.03, 0.01, and 0.004 min^{-1}) could be the factor responsible for the variability of the interpretation reported in the literature. Low reversal rates will lead to inhibition that may be interpreted as near irreversible, depending on the time allowed for recovery. For example, the reversal rate of 0.03 min^{-1} found when *Mt*AHAS is inhibited by PS will lead to recovery of 95% of the activity after about 100 min, whereas for *Sc*AHAS inhibited by BSM ($k_3 = 0.004$ min^{-1}), an equivalent recovery takes about 13 h. Clearly, the amount of enzymatic activity recovered will depend on the period of time allowed for exchanging the inhibited enzyme into inhibitor-free buffer.

This study validates the theory proposed by Schloss[3,8] with the exception that the inhibition does not appear to be irreversible. The mechanism of accumulative inhibition by AHAS inhibitors is novel and helps to explain their potent herbicidal activity. The design of new AHAS inhibitors, either as advanced herbicides or new antimicrobials, should include investigations aimed at determining contributions resulting from oxidative inactivation of this enzyme to maximize accumulative inhibition.

Acknowledgements

Crystallization and preliminary X-ray data were measured at the University of Queensland Remote-Operation Crystallization and X-ray diffraction facility (UQROCX). The final

measurements were made at the Australian Synchrotron. The views expressed herein are those of the authors and not necessarily those of the owner or operator of the Australian Synchrotron. This work was supported by the NHMRC (grant 1008736), and by an ARC fellowship to C.M.W. (FT10100851).

Keywords: accumulative inhibition · enzymes · herbicides · kinetics · structure elucidation

How to cite: *Angew. Chem. Int. Ed.* **2016**, *55*, 4247 – 4251
Angew. Chem. **2016**, *128*, 4319 – 4323

[1] R. F. Sauers, G. Levitt, in *Pesticide synthesis through rational approaches*, *Vol. 255* (Eds.: P. Magee, G. Kohn, J. Menn), American Chemical Society, Washington DC, **1984**, pp. 21 – 28.
[2] a) R. G. Duggleby, S. S. Pang, *J. Biochem. Mol. Biol.* **2000**, *33*, 1 – 36; b) D. M. Chipman, R. G. Duggleby, K. Tittmann, *Curr. Opin. Chem. Biol.* **2005**, *9*, 475 – 481; c) R. A. LaRossa, J. V. Schloss, *J. Biol. Chem.* **1984**, *259*, 8753 – 8757.
[3] D. M. Chipman, J. V. Schloss, in *Biosynthesis of Branched Chain Amino Acids* (Eds.: Z. Barak, D. M. Chipman, J. V. Schloss), Balaban Publishers, Weinheim, **1990**, pp. 329 – 356.
[4] J. Durner, V. Gailus, P. Boger, *FEBS Lett.* **1994**, *354*, 71 – 73.
[5] a) A. Berkessel, S. Elfert, V. R. Yatham, J.-M. Neudörfl, N. E. Schlörer, J. H. Teles, *Angew. Chem. Int. Ed.* **2012**, *51*, 12370 – 12374; *Angew. Chem.* **2012**, *124*, 12537 – 12541, and references therein; b) D. Meyer, P. Neumann, E. Koers, H. Sjuts, S. Ludtke, G. M. Sheldrick, R. Ficner, K. Tittmann, *Proc. Natl. Acad. Sci. USA* **2012**, *109*, 10867 – 10872.
[6] A. K. Chang, R. G. Duggleby, *Biochem. J.* **1997**, *327*, 161 – 169.
[7] Y. T. Lee, C. J. Cui, E. W. Chow, N. Pue, T. Lonhienne, J. G. Wang, J. A. Fraser, L. W. Guddat, *J. Med. Chem.* **2013**, *56*, 210 – 219.
[8] J. V. Schloss, in *Herbicides inhibiting branched chain amino acid biosynthesis*, *Vol. 10* (Ed.: W. Ebing), Springer, Berlin, **1994**, pp. 3 – 81.
[9] a) L. M. Abell, J. V. Schloss, *Biochemistry* **1991**, *30*, 7883 – 7887; b) J. M. T. Tse, J. V. Schloss, *Biochemistry* **1993**, *32*, 10398 – 10403.
[10] K. Tittmann, K. Schroder, R. Golbik, J. McCourt, A. Kaplun, R. G. Duggleby, Z. Barak, D. M. Chipman, G. Hubner, *Biochemistry* **2004**, *43*, 8652 – 8661.
[11] S. S. Pang, L. W. Guddat, R. G. Duggleby, *J. Biol. Chem.* **2003**, *278*, 7639 – 7644.
[12] a) J. Durner, V. Gailus, P. Boger, *Plant Physiol.* **1991**, *95*, 1144 – 1149; b) F. Ortega, J. Bastide, T. R. Hawkes, *Pestic. Biochem. Physiol.* **1996**, *56*, 231 – 242.

Received: December 29, 2015
Revised: January 22, 2016
Published online: February 29, 2016

